

The Effect of Machining on Surface Integrity of Gamma Titanium Aluminides Using Different Cemented Carbide Tools



S. D. Castellanos, J. Lino Alves, R. Neto and A. Cavaleiro

Abstract Gamma titanium aluminides are a new generation of light materials that compete with nickel or cobalt superalloys, when it comes to the manufacture of very high resistance requirement components such as low and high-pressure compressor blades, in the case of aeronautical applications. Machining is a process used to manufacture such components. However, in available literature, the specific information regarding machining performance of gamma titanium aluminides is scarce. The present research focused on the comparative study of the performance of coated tungsten carbide (WC-Co) inserts with round geometry in face milling operation of a gamma titanium aluminide alloy (Ti-48Al-2Nb-0.7Cr-0.3Si). Six different cutting-inserts in a combination of three different compositions of WC-Co substrates and two edge-geometries (XL and XM) recommended for conventional titanium alloys were tested. Milling experiments were carried out for different cutting speed, depth of cut and chip thickness. The results are discussed in terms of the correlation between cutting parameters with cutting force, surface roughness and work-hardening. The study showed that chip thickness, significantly affected the machined surface integrity in related with the tool insert geometry. Insert type C-XL showed better performance for cutting speed to 45 m/min, while inserts types A-XL and B-XM showed better behavior for cutting speed to 70 m/min.

Keywords Machinability · Gamma titanium aluminides · Surface integrity
Coated tungsten carbide tools

S. D. Castellanos (✉) · J. Lino Alves · R. Neto · A. Cavaleiro
Faculdade de Engenharia da Universidade do Porto, INEGI, Rua Dr. Roberto Frias, 4200-465
Porto, Portugal
e-mail: sdcastellanos@espe.edu.ec

S. D. Castellanos
Universidad de las Fuerzas Armadas - ESPE, Av. General Rumiñahui, P.O. Box 171-5-231B,
Sangolquí, Ecuador

© Springer Nature Switzerland AG 2019
L. F. M. da Silva (ed.), *Materials Design and Applications II*, Advanced
Structured Materials 98, https://doi.org/10.1007/978-3-030-02257-0_26

1 Introduction

Machining of titanium aluminide-based alloys is considered by several authors [1–5] as a challenge. This is due to their mechanical properties (ductility, specific strength, low thermal conductivity and mechanical resistance at elevated temperatures) which leads to an unusual response pattern to the cutting process causing surface and sub-surface defects. The main drawbacks on the workpiece surface (feed marks, smearing, tearing surface, surface cracks, lay patterns) are mainly due to the uncertain selection of machining parameters (cutting parameters, tool material, tool geometry, cutting environment) [6–9]. Several authors [8, 10–14] agree that the lack of studies on the machining performance of titanium aluminides-based alloys (cutting parameters, optimization of tool geometry and material) is still one of the main factors limiting the growth of their industrial application.

Cutting tools and cutting parameters are the most important factor affecting the machining operation. The machining of titanium aluminides induced thermal and mechanical effects on the cutting tool that can affect its working life [15–17]. The combination of high cutting force and high temperature in the cutting area during the machining of these materials causes the tool edges to plastically deform or break by chipping. Also, it has been shown that from the perspective of surface integrity and productivity in the machining of titanium aluminides it is more difficult to optimize the performance of cutting tools [18, 19].

In the machining of titanium aluminides, cemented tungsten carbide tools are the most studied by researchers. Several types of tool wear mechanisms were reported during the cutting process [13, 20–22]. However, coated or uncoated WC cutting tools are the primary choice for machining titanium aluminides, carbide tools use single or multi layers coating of Aluminum Oxide (Al_2O_3), Titanium Nitride (TiN), Titanium Carbide (TiC), Titanium Carbo-Nitride (TiCN) or Titanium Aluminum Nitride (TiAlN) in order to protect the tool from wear and improve tool performance.

There are several defects that affect the quality of surface integrity in titanium aluminides, the main ones being cracks, lamellar deformation, work-hardening, smearing between other. These types of defects have been observed by different researchers [3, 18, 23–25] and are affected by the characteristics of the cutting tool and the cutting parameters. Surfaces cracking showed proportional to the flank wear on the cutting tool and influenced by the low ductility of these alloys [5]. Low thermal conductivity leads to increase temperatures on the cutting edge and promote the flank wear on the tool's cutting edge.

On the other hand, several studies on the integrity of the machined surface have been carried out using cemented tungsten carbide (WC) tools with and without coating [15, 18, 19, 22, 25, 26]. Based on these investigations it is observed that surfaces produced with WC tools show a greater tendency to surface cracking compared to the use of other tools such as polycrystalline cubic boron nitride (PCBN), polycrystalline diamond (PCD) and cubic boron nitride (CBN) [1].

The main disadvantages of the microstructure by the machining process in titanium aluminides is the plastic lamellar deformation. This behavior is indicative of

the ability of this material to keep the mechanical strength at high temperatures and low ductility [1, 27]. Researchers such as Mantle, Aspinwall and their research teams [5, 19, 23, 24] have studied these effects and demonstrated that several factors such as cutting parameters (cutting speed, feed rate and cutting depth), tool parameters (geometry, material, coating, wear) and part parameters (material composition, grain size) influence the tendency of plastic lamellar deformation in these materials.

On the other hand, in the machining of titanium aluminides reduction in tool wear decrease the depth of surface alterations (from 30 to 10 μm) [3]. This indicates that the cutting conditions are important factors and that high temperatures and tool wear are also important factors for lamellar plastic deformation.

The work-hardening tendency is strongly influenced by the low deformation capacity of titanium aluminides alloys. This surface hardness can increase up to 65% of its initial hardness (bulk material), with a depth of up to 50 μm after the first cutting pass [24]. Based on the results analysed in most of the conducted research [15, 24, 28, 29], it is possible to conclude that there is no evidence hardened layers greater than 250 μm , and peak values reached at a maximum depth of 50 μm and it is observed that the thermal softening effect is less than the work-hardening effect in these alloys. It is for this that the effect of the surface hardening is improving by the cutting tool.

Machinability of titanium aluminides can be researched from multiple approaches and cutting forces values are one of the main data that provide comprehensive information about the machining process, thus contributing to better understanding of the machinability of these alloys. It has been reported by some publications [21, 30] that the cutting forces in machining titanium aluminide-based alloys are considerably higher than in other titanium-based alloys such as Ti-6Al-4V ($F_a = +200\%$, $F_r = +200\%$, and $F_t = +130\%$) or Ti-6Al-2Zr-1Mo-1V ($F_a = +200\%$, $F_r = 190\%$ and $F_t = 180\%$). The experimental results show that the energy used for machining titanium aluminides based alloys is approximate ~5 times higher than that of conventional titanium alloys [11, 16, 31].

For the improvement of the surface integrity of workpieces, an analysis of the material cutting process is the starting point for an adequate study of cutting tools and cutting parameters to obtain the expected results.

In order to study the machinability of gamma titanium aluminide alloys, the aims of this paper were to investigate the performance of six coated cemented carbide tools with round geometry under a range of cutting parameters (cutting speed, depth of cut and chip thickness) for face milling operations. Milling experiments are presented and discussed in terms of cutting forces, work-hardening, and roughness.

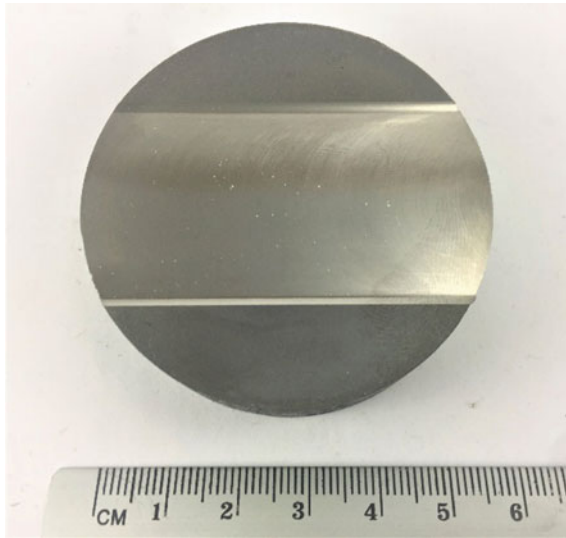


Fig. 1 Cutted EDM and machined sample

2 Experimental Procedure

2.1 Workpiece Material

The material used in this work is a γ -titanium aluminide (Ti-48Al-2Nb-0.7Cr-0.3Si at.%) produced by GfE Metalle und Materialien GmbH (Nuremberg, Germany) via VAR skull melting. Samples were cut out of a 55 mm diameter bar using a (machine name) electrical discharge wire machine (EDWN). Also, axial and radial specimens of the machined samples were cut to perform the metallographic analysis. The machined and non-machined sample is illustrated in Fig. 1.

The metallographic test samples were hot mounted in bakelite in a Struers Prontopress-2 mounting press, ground and polished in a semiautomatic polishing machine at 150 rpm (Struers Planopol-3). The process began with sandpaper numbers 80, 320, 600, 1000 and 1200, and polished in a cloth with $0.01 \mu\text{m}$ alumina and a solution of hydrogen peroxide (H_2O_2). Polished samples were chemically etched with Kroll reagent (1 ml of hydrofluoric acid, 3 ml of nitric acid and 500 ml of water).

The microstructural analysis was performed using an optical microscope Zeiss Axiophot. Characteristic images taken at 150X and 23X (Fig. 2) reveals a near gamma lamellar microstructure consisting of γ (TiAl) and α_2 (Ti_3Al)- γ (TiAl) phases with a different orientation of lamellae. No significant alterations of the microstructure were detected both in the axial than in the radial direction of the samples.

The chemical composition of the alloy is listed in Fig. 3, while the main properties at room temperature are reported in Table 1. Furthermore, a tensile test was performed

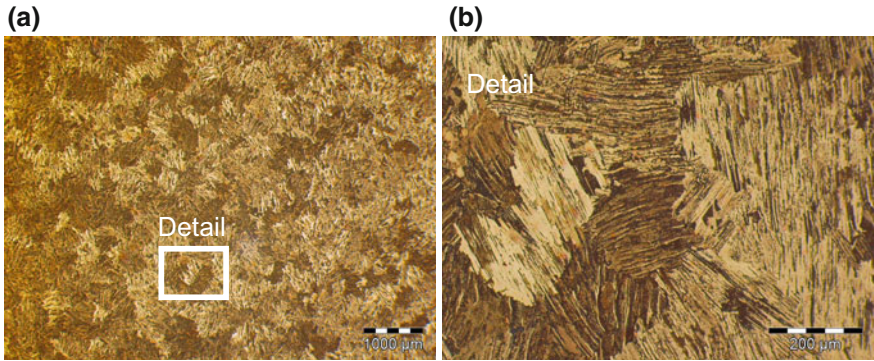


Fig. 2 Microstructure of γ -titanium aluminide (Ti-48Al-2Nb-2Cr-0.3Si at.%)

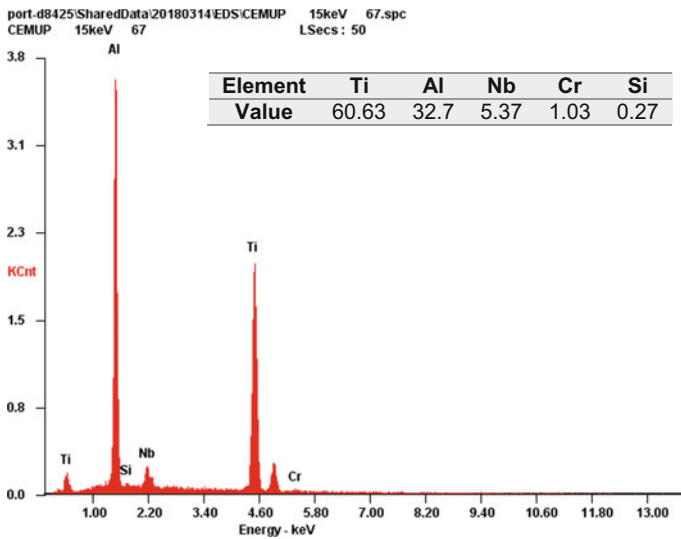
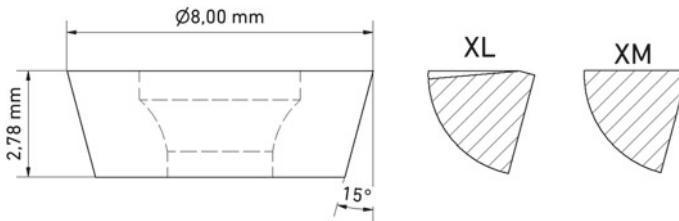


Fig. 3 Chemical composition of workpiece material (wt%)

in accordance with the EN 10002-1 standard, by means of a MTS 810 testing machine and the elongation was measured with a mechanical extensometer MTS 634.25F-24. Specimens of 3 mm in thickness were cut out from a material bar. The tests were conducted at a test speed of 0.25 mm/min until a tensile failure occurred. Workpiece hardness was measured before machining test, by a Wolpert Dia Testor 2Rc universal hardness tester, according to HV40 test condition, the hardness showed an average hardness of 275 HV40 (with a standard deviation of 5 HV40).

Table 1 Mechanical properties of tested titanium aluminide [32]

Mechanical properties	Value
Density (g/cm^3)	3.95
Hardness (HV10)	285
Young Modulus at RT (GPa)	155
Young Modulus at 800 °C (GPa)	102
Ultimate tensile strength (MPa)	530
0, 2 Yield strength (MPa)	464
Melting temperature (°C)	1605

**Fig. 4** Cutting insert and edge geometries

2.2 Cutting Tool Material

In order to investigate the influence of the cutting tool on the workpiece surface on γ -TiAl, comparative trials were carried out with a fine grain (grain size $<1 \mu\text{m}$) carbide insert. Tool selection was based on the previous researches [24, 29, 33, 34] and the recommendations of the tool manufacturers for titanium alloys. An indexable milling cutter for face milling operation with double positive geometry and $\varnothing 35 \text{ mm}$ for round cutting inserts were used in this study. Round cutting inserts with $\varnothing 8 \text{ mm}$ of two different cutting-edge geometries (Fig. 4) and three substrate cemented carbide compositions are analyzed in the present study. Carbide insert characteristics are shown in Table 2.

2.3 Machining Tests

Machining tests were performed on a five-axis CNC milling machine DeckelMaho Mori Seiki DMU 60 eVo, with a Heidenhain iTNC530 controller with a maximum spindle speed of 18.000 RPM, drive power of 25 HP and 50 m/min of maximum feed rate. The experimental trial uses finishing cutting parameters and high-pressure coolant (HPC) lubrication conditions with 6% emulsion of AVILUB METACOOOL BFH oil miscible in water supplied at a 70 bar of pressure through spindle coolant

Table 2 Cutting insert specifications (Tool geometry and materials)

Designation	A-XL	A-XM	B-XL	B-XM	C-XL	C-XM
<i>Substrate characteristics</i>						
Hardness (HV)	~1900	~1900	~1650	~1650	~1550	~1550
Coating	PVD (Ti, Al) N ₂					
<i>Geometry characteristics</i>						
Rake angle	5°	0°	5°	0°	5°	0°
Rake land angle	15°	0°	15°	0°	15°	0°
Clearance angle	15°					

Table 3 Cutting parameters for the experimental work

Taguchi orthogonal array L4			
Test	Cutting speed (m/min)	Axial depth (mm)	Hex (mm)
Trial 1	70	0.3	0.03
Trial 2	70	0.5	0.04
Trial 3	45	0.3	0.04
Trial 4	45	0.5	0.03

supply. These cutting conditions were chosen according to previous research studies and recommendations of the tool’s manufacturers [3, 9, 11, 16, 19, 35, 36].

Taguchi’ DOE approach was adopted to reduce the number of trials. The experimentation was based on Taguchi’s L4 orthogonal array and was performed by each cutting insert type. Test matrix with three factors and two levels of cutting parameters with four trials by cutting inserts are being considered. Three repetitions of each experimental trial have been performed, and the tests were executed following a random order. The specific cutting parameters and orthogonal array are given in Table 3. The radial depth of cut was kept constant (full engagement arc). Collected data were statistically evaluated using the analysis of means which was performed using Minitab software.

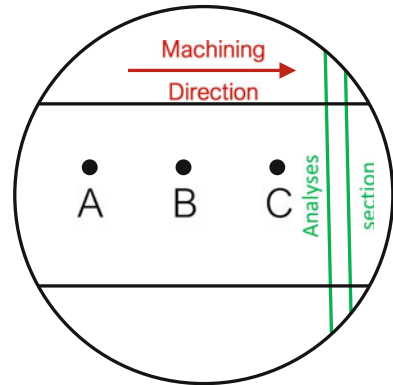
2.4 Cutting Force and Surface Integrity Testing

Cutting force tests were carried out by a four-component piezo-electric dynamometer Kistler 9272 mounted on the worktable and connected to a charge amplifier Kistler 5070A. The amplified cutting forces signal was acquired in a computer with an Advantech USB 4750A data acquisition card capable of the testing rate at 800 Hz. Figure 5 shows the machining setup of the experiment.



Fig. 5 Experimental setup

Fig. 6 Machining workpiece cutting section used for the analysis



The surface roughness was measured by A 3D digital MICROSCOPE Bruker Nplex, with a standard lens of 10X, with an optical resolution of $0.9 \mu\text{m}$. Sampling surface area of measuring was $250 \mu\text{m} \times 250 \mu\text{m}$. Three zones 130 mm from each other along the milling direction on the surface were selected to obtain the roughness average (Points A, B, and C in Fig. 6). Surface hardness was measured by the same hardness tester used to measure the bulk material, according to HV40 test condition. Indentations were performed next to roughness measurement area. Surface hardness values showed an average of these three points.

3 Results and Discussions

The results and discussion are focused on the workpiece surface integrity on the finishing procedures when milling Ti-48Al-2Nb-2Cr-0.3Si with six different cutting tools. The results obtained by each insert are cutting forces, work-hardening, roughness and surface defects.

3.1 Cutting Forces and Surface Integrity Analysis

The discussion in this study is focused on the effect of cutting parameters (Cutting speed, depth of cut and chip thickness) in the cutting forces and the surface integrity when milling titanium aluminides. The test was performed on a workpiece with no surface discontinuities to avoid the correlation of the cutting forces with the depth of cut variation. Moreover, these tests have been carried out by full engagement operation in order to obtain a complete cutting force waves and continuous cutting-edge contact for analysis purposes. In all trials, a full new insert was used.

The tests are conducted using a single cutting insert to avoid the effect of runout. The feed rate per revolution to reflect the single insert cutting was adapted in the NC program. Also, toolpath trajectory to prevent higher cutting forces at the cutting entrance tool wear and vibration have been programmed. The comparative analysis of the cutting forces was conducted at a zone on 40 mm from the start cutting point (Fig. 7). The results indicate that in general terms the Fz force (axial force) is the dominant force component, being approximate ~1.5 and ~1.7 times that of the Fx and Fy, respectively. since the variation between Fz, Fx and Fy follow the similar trend in all the tests. The discussion about cutting forces was focused on resultant cutting force (Fr).

3.1.1 Influence of the Cutting Speed

Cutting speed is the main cutting parameter. Considering the low ductility and brittle nature of titanium aluminides, was expectable that the cutting inserts with neutral XM geometry would produce higher cutting forces than the XL geometry. However,

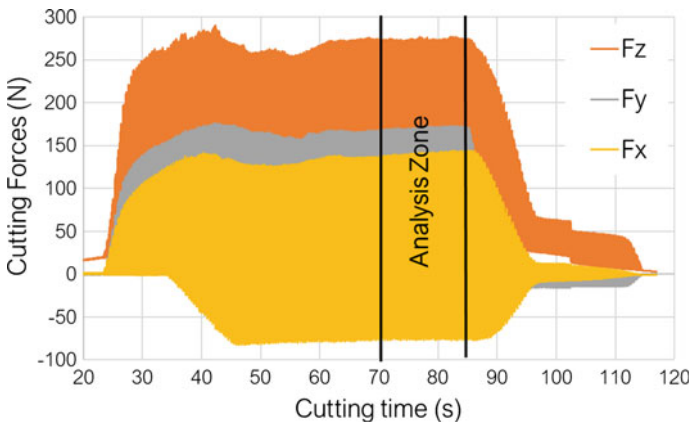


Fig. 7 Cutting forces profile on machining of RNT 650 at $V_c = 70$ m/min, $a_p = 0.5$ mm and $hex = 0.04$ mm with A-XL cutting insert

Table 4 Increase of the cutting forces according to the depth of cut variation

Cutting inserts	Hardness of cutting insert (HV40)	Cutting forces with Vc = 45 m/min	Cutting forces with Vc = 70 m/min	Cutting force variation	
		(N)	(N)	(N)	(%)
A-XL	1900	355.00	354.00	-1.00	0.3
A-XM	1900	381.00	392.00	11.00	2.9
B-XL	1650	364.00	409.00	45.00	12.4
B-XM	1650	351.00	350.00	-1.00	0.3
C-XL	1550	318.00	564.00	246.00	77.4
C-XM	1550	384.00	845.00	461.00	120.1

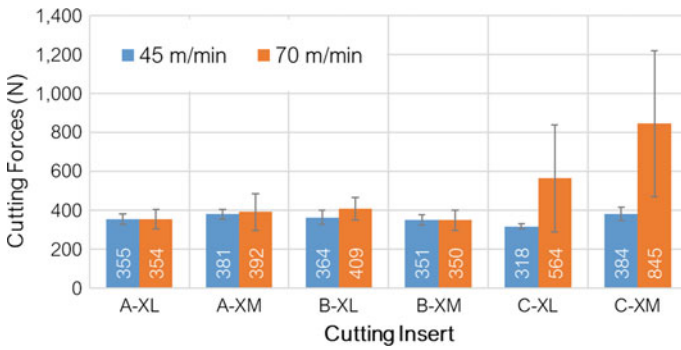


Fig. 8 Effect of the cutting speed in the resultant cutting force

a non-significant difference was found between both geometries mainly for A and B insert types (Table 4).

The effect of variation of the cutting speed on the cutting forces for each individual insert is shown in Fig. 8. As can be seen for cutting inserts B, cutting forces for XL geometry are 6.3% higher than XM, while that with A inserts, the cutting forces were 1.6% lower for the XL geometry. This behavior is attributed to the combination of the substrate properties (composition, hardness) and the cutting-edge geometries. Also, C cutting inserts show a similar performance to A insert. This allows us to determine a tendency of the XL geometry to present lower cutting forces. For B cutting inserts, it is not possible to define a similar trend than for A and C inserts.

The considerable difference showed for C cutting inserts at cutting speed of 70 m/min was caused by early wear under this cutting condition. It has been demonstrated that for C-XM insert use of cutting speed of 70 m/min was catastrophic regardless of the depth of cut or chip thickness selected. However, for C-XL insert, wear was only observed after 40 s of cutting using cutting conditions of Vc = 70 m/min, ap of 0.5 mm and hex = 0.04 mm, (Fig. 9).

On the other hand, cutting speed of 45 m/min regardless of the depth of cut or chip thickness was the best performance for all the inserts in terms of cutting forces.

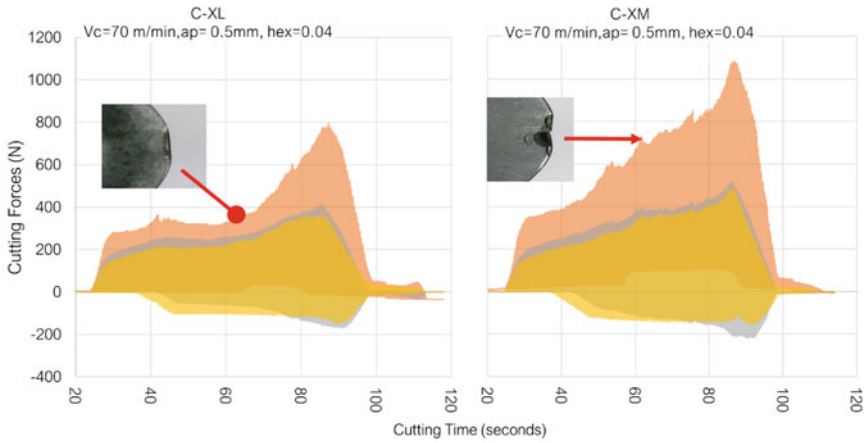


Fig. 9 Cutting forces profiles for cutting insert C-XL and C-XM

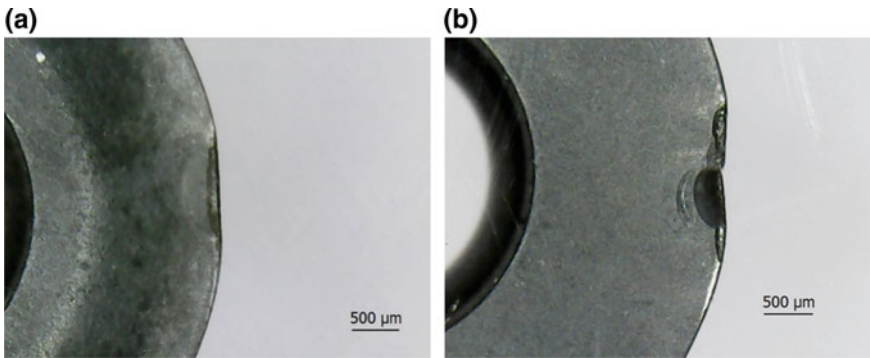


Fig. 10 Cutting inserts. **a** C-XL geometry and **b** C-XM geometry

On the other hand, wear on the cutting edge of C cutting inserts demonstrate the characteristic abrasive wear caused when machining titanium aluminides [13]. Cutting forces profile for C-XM cutting insert has a constant growth (Fig. 9) indicates the progressive tool wear, which leading the cutting-edge fracture (Fig. 10b). While for XL geometry at $V_c = 70$ m/min, $a_p = 0.5$ and hex 0.04 mm the flank wear after 35 s was of $50 \mu\text{m}$ (Fig. 10a). On A and B cutting inserts with both geometries, no significant wear (less than $10 \mu\text{m}$) was observed.

In terms of surface integrity, all machined surface showed a hardened layer in response to the chip cutting process, demonstrating work hardening tendency. Figure 11 shows the hardness increment according to the cutting forces. A hardness increment between 29 to 39 HV40 are present for cutting forces from 300 to 400 N. Likewise, it can be observed that work hardening is sensitive to the variation of cutting forces.

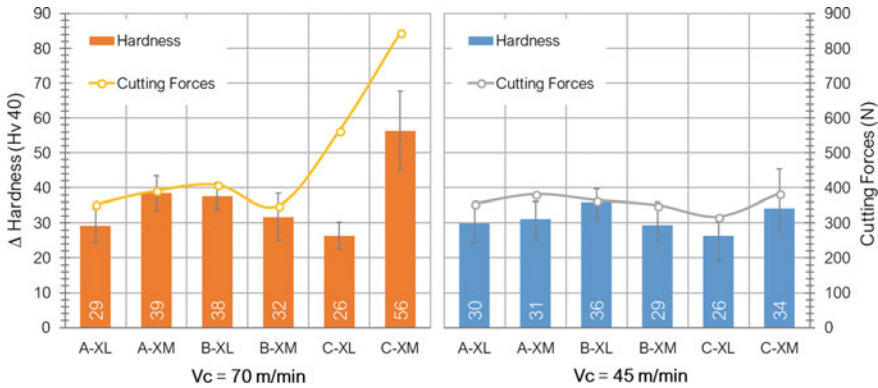


Fig. 11 Surface hardness increment according to cutting forces and cutting speed on TiAl alloy

Where the sensitivity of the material by the fracture of the cutting edge of the C-XM insert is highlighted, which causes a greater increase in surface hardness. This is probably due to the greater deformation that would occur in the cutting area caused by the notches on the cutting edge. However, an unexpected result was caused by the C-XL insert, which showed a lower increase in hardness, even in the presence of cutting-edge wear. This behavior could be indicated by the decrease in the depth of cut caused by the cutting-edge wear that affects the depth of the surface work hardening.

With regard to the geometries, there are no significant differences that allow us to conclude an effect of these geometries for work hardening in this range of cutting conditions.

For surface roughness, the results are presented in Fig. 12. A decrease of ~17.5% in the surface roughness was observed when the cutting speed increase 55%. All surface roughness values measured for the experimental trials were less than 0.450 μm, including those obtained with worn inserts (C-XL and C-XM) at cutting speed of 70 m/min. Demonstrating surface roughness values suitable for applications with demanding surface specifications [1].

Use of round geometry (nose radius 4 mm) shows that it has advantages for machined surface of titanium aluminides thanks to the larger contact area. With reference to the effect of both cutting speed and nose radius, it is important to note that the values obtained by cutting inserts A-XL and B-XM are similar to those obtained by authors such as [3, 22, 30], which reports average roughness values of 0.250 μm at cutting speeds of 120 m/min in milling and turning operations for some cases also with cryogenic cooling conditions. Considering the performance of these two inserts, it would be expected that at cutting speeds higher than 70 m/min lower roughness values could be obtained.

On the other hand, XL and XM cutting edge geometries improve surface roughness by 20% and 15% respectively, when cutting speed increases from 40 m/min to

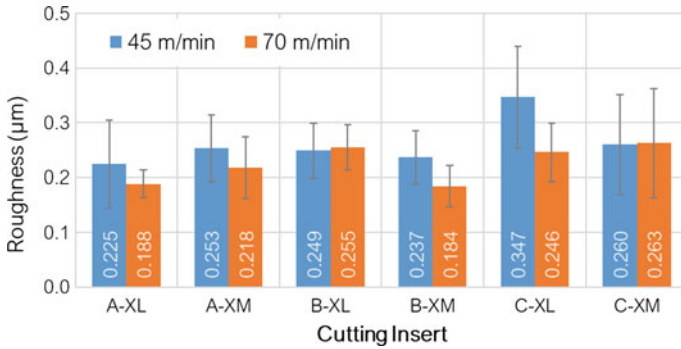


Fig. 12 Effect of cutting speed in surface roughness (in feed directions)

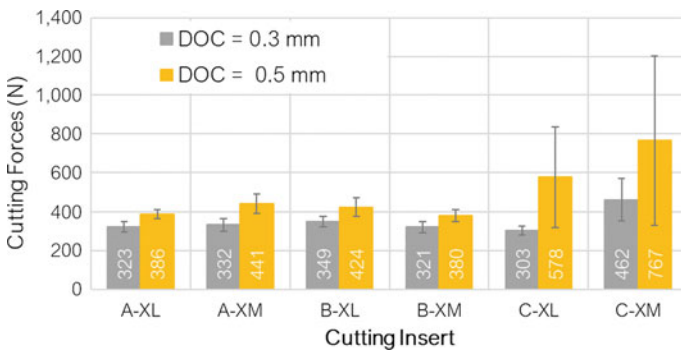


Fig. 13 Effect of depth of cut in the resultant cutting forces

70 m/min. Based on this difference, it can be concluded that cutting inserts with XL geometry provide slightly better performance than XM.

3.1.2 Influence of the Depth of Cut

The depth of cut is usually the most influential factor for machining of any material. This is due to the effect it has on the removal rate of material. For cutters with round cutting inserts, the variation of the cutting depth has a different performance than straight-edged inserts. This is due to the orientation of the cutting forces. A deeper depth of cut for these inserts increases the angle of entry (K_r), orienting the cutting forces towards the spindle and improving the stability of the cutting process. In addition, the cutting depth in this round geometry varies the effective cutting diameter (D_{cap}) that modifies the material removal rate. Figure 13 shows the results for depth of cut.

The data obtained indicate an expected reaction, where the greater cutting depth increases the cutting forces. For this case, as well as in the analysis of cutting speeds,

Table 5 Increase of the cutting forces according to the depth of cut variation

Cutting inserts	Hardness of cutting insert (HV40)	Cutting forces with DOC 0.3 mm	Cutting forces with DOC 0.5 mm	Cutting force increase	
		(N)	(N)	(N)	(%)
AXL	1900	322.62	386.46	63.83	19.8
AXM	1900	332.36	440.94	108.58	32.7
BXL	1650	348.73	424.35	75.63	21.7
BXM	1650	320.52	379.93	59.41	18.5
CXL	1550	303.48	578.41	274.93	90.6
CXM	1550	461.78	766.61	304.84	66.0

the inserts with substrates A and C indicate lower cutting forces with XL geometry. Whereas for XM geometry the B substrate caused the lowest resultant cutting force. Table 5 shows the increases in cutting force in response to the increase in the depth of cut (60%).

As can be appreciated, the C cutting inserts were more sensitive to this variation as a result of their hardness (1550 HV). However, an increase of 100 HV and 350 HV in hardness for the B and A cutting insert respectively, substantially improved the performance of the cutting tools. This response of the material to the hardness of the inserts suggests that the connection between the cutting-edge geometry and the material has a strong influence on cutting forces [37]. As can be seen from the behavior of the A-XL and B-XM inserts.

Nevertheless, the higher hardness of the A cutting inserts does not exhibit the best performance of the experimentation. It was the A-XL and B-XM inserts that showed the best performance in this range of cutting conditions.

With regard to the work hardening of the surface, a deeper cutting depth generally results in a thinner hardened layer of the machined surface. This behavior is observed in Fig. 14. In terms of hardness variation, all inserts have a homogeneous performance with a maximum variation of 5 HV. However, for the tendency to surface hardening, the C-XL cutting insert has the lowest value but not too far from the other cutting tools. This indicates that the depth of cut for finishing operations with toroidal geometry tools would not have a significant impact on the hardening tendency of TiAl. In addition, the use of a low DOC, contrary to expectations, leads to a higher surface hardening effect and probably a thicker hardening layer. This concept will be analyzed in greater detail in future studies with varying cutting conditions and insert diameters.

With reference to surface roughness, Fig. 15 shows the results obtained. As expected the variation in depth of cut does not cause any noticeable response in surface roughness. The variations observed between cutting depths for each insert are very slight, with exception of A-XL insert which reduces roughness by 25% at a depth of 0.5 mm.

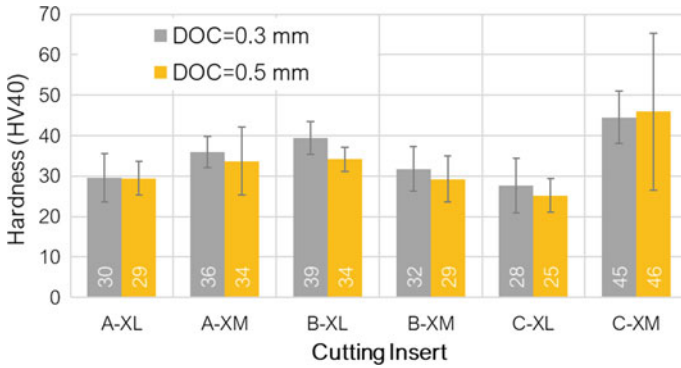


Fig. 14 Surface hardness increment according to cutting forces for DOC of 0.3 and 0.5 on TiAl alloy

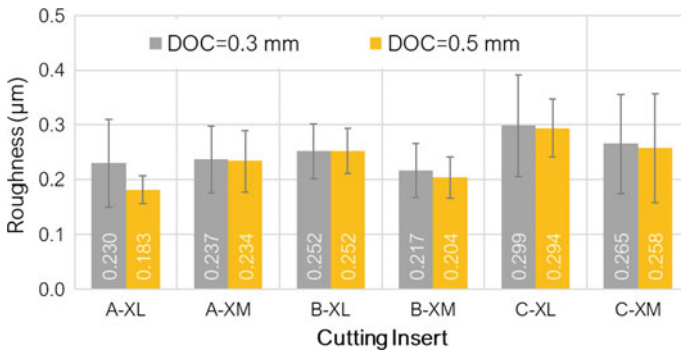


Fig. 15 Effect of depth of cut in surface roughness (in feed directions)

3.1.3 Influence of the Chip Thickness

As for the cutting forces, it is normal for them to increase in proportion to the amount of cutting material. Therefore, depth of cut and feed rate are the parameters that most affect this variation.

On the other hand, the feed rate of the cutting tool is strongly related to the geometry and thickness of the chip that is formed in the cutting process. In the case of inserts with round geometry, the chip thickness (h_c) varies according to the cutting depth and the angle entered, which allows increasing the feed rate. Consequently, this variable was selected as the reason for the study instead of the advance.

The effect of chip thickness on cutting forces was higher to presented at the depth of cut. A considerable increase in cutting forces occurred with an increase of only 0.01 mm in chip thickness demonstrating more sensitivity to this variable. As shown in Fig. 16, cutting insert BXM presents the best combination of variation and magnitude of cutting forces. In addition, the cutting forces caused by XL geometry

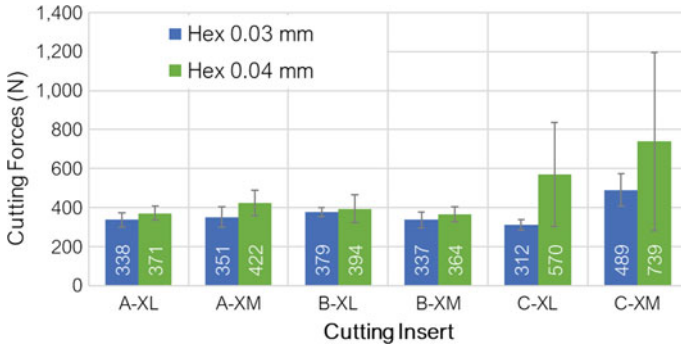


Fig. 16 Chip thickness effect in the resultant cutting forces

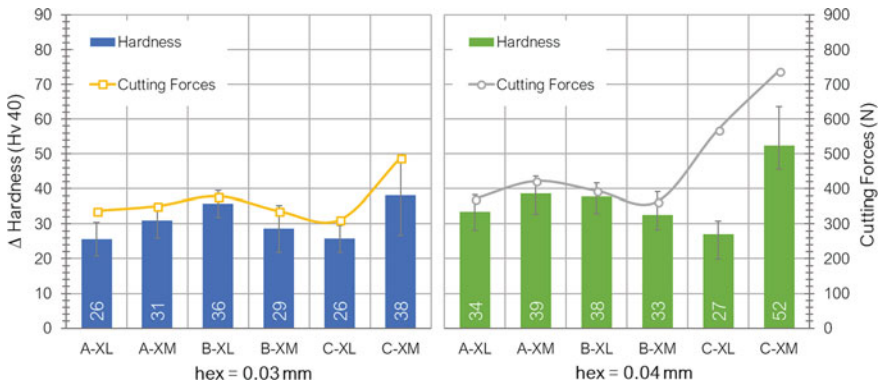


Fig. 17 Surface hardness increment according to cutting forces and chip thickness on TiAl alloy

cutting inserts tend to vary less than those of XM geometry due to chip thickness variation.

For work hardening, a homogeneous variation between the cutting forces and the increase of the surface hardness is achieved, especially with a chip thickness of 0.03 mm. Variation in hardening has the opposite behavior to that of the depth of cut, in this case, a greater amount of material removed (hex = 0.04) promotes growth in surface hardness (Fig. 17).

As expected, chip thickness is the main factor affecting surface roughness. As shown in Fig. 18 the results obtained in terms of arithmetic mean roughness Ra for each tested cutting inserts. The A and B cutting inserts with both geometries cause roughness values that do not exceed 350 m, while for C inserts the values reach ~450 m. With regard to the performance of the C-XL geometry, this indicates that initial wear of the cutting edge does not strongly affect the surface finish due to the increased radius of the cutting edge. With the C-XM insert, the breakage of the cutting edge affects the surface roughness to a greater extent. This is also compatible

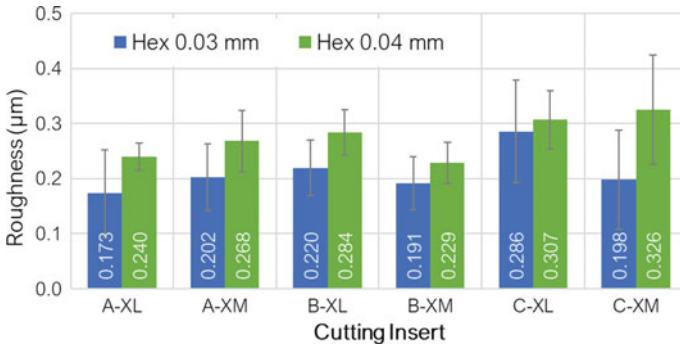


Fig. 18 Effect of chip thickness in surface roughness (in feed directions)

Table 6 Increase of the surface roughness according to the chip thickness variation

Cutting inserts	Hardness of cutting insert (HV40)	Roughness with hex 0.03 mm	Roughness with hex 0.04 mm	Roughness increase	
		(µm)	(µm)	(µm)	(%)
AXL	1900	0.173	0.240	0.067	38.7
AXM	1900	0.202	0.268	0.066	32.7
BXL	1650	0.220	0.284	0.064	29.1
BXM	1650	0.191	0.229	0.038	19.9
CXL	1550	0.286	0.307	0.021	7.3
CXM	1550	0.198	0.326	0.128	64.6

with the results obtained by [18]. However, the roughness values of the C-XL insert are higher than those of the other inserts.

The results in terms of roughness variation listed in Table 6 highlight that a 0.01 mm difference in chip thickness causes a 20–60% increase in surface roughness for almost all cutting inserts. An exception was the C-XL insert which varies by 7% for the reasons explained above. In terms of geometries, there is a slight tendency of XL geometry to affect roughness in response to the increase in chip thickness. As a result, the surface roughness is more affected by the 0.01 mm variation in chip thickness than by the 25 m/min cutting speed or the 2 mm cutting depth.

3.1.4 Surface Defects

As has been previously commented, the machining of titanium aluminide alloys leads to an unusual response pattern to the cutting process causing surface and sub-surface defects such as feed marks, smearing, surface cavities and cracks [1, 6–9, 33]. The surface integrity defects confirmed are strongly linked to cutting speed, feed rate, depth of cut, tool geometry, rake angle, nose radius among other. Optical and SEM

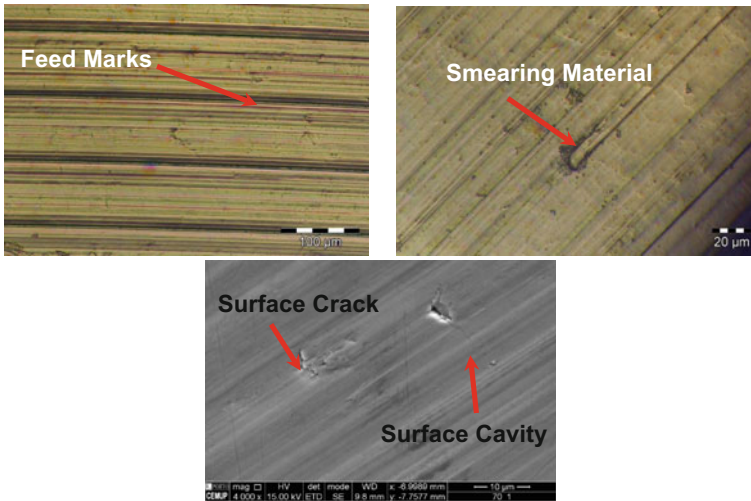


Fig. 19 Surface defect feed marks, smearing, surface cracks and cavities on machined surfaces

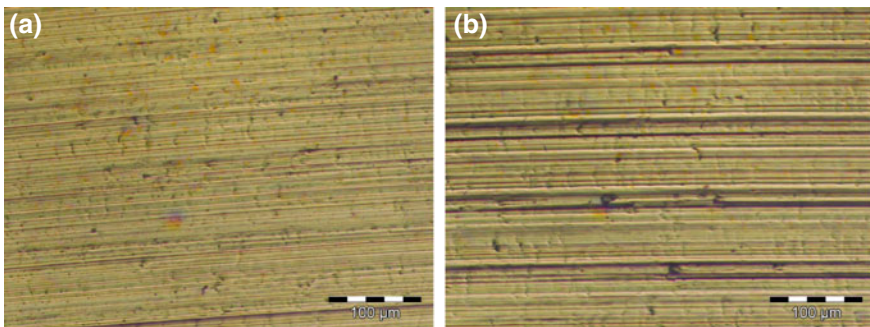


Fig. 20 Machined surfaces with C-XL cutting insert at $V_c = 70$ m/min. **a** $DOC = 0.5$ mm and $hex = 0.04$ mm, **b** $DOC = 0.3$ mm and $hex = 0.03$ mm

observation on the machined surfaces around the hardness and roughness analyzed area was conducted. The surface observation of the machined samples showed several defects that confirmed the results presented in the surface integrity analyses (Fig. 19).

All specimens showed some defect. Considering the analyzed range of machining parameters for all inserts, the combination of cutting speed of 70 m/min, depth of cut of 0.5 mm and chip thickness of 0.04 mm, exhibited a tendency to cause feed marks, surface cracks, and material smearing. In contrast to this trend, the surfaces machined with the same cutting speed but with the depth of cut of 0.3 and a chip thickness of 0.03 showed a lower number of defects. This behavior would demonstrate that the effect of cutting speed on the surface defect formation is less than the material removal rate (Fig. 20).

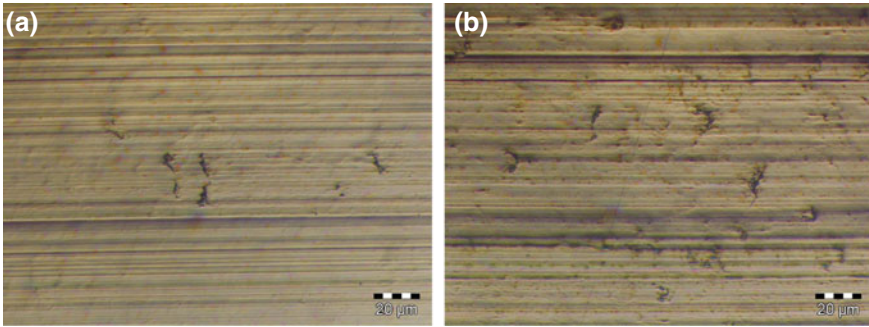


Fig. 21 Machined surfaces at $V_c = 70$ m/min, $DOC = 0.3$ mm and $hex = 0.03$ mm with **a** worn cutting insert C-XL and **b** broken cutting-edge C-XM

It was also evident that the fracture of the cutting edge of the C-XM insert generated the worst quality surface. On the other hand, the C-XL insert has a more homogeneous and smooth surface. Caused by cutting edge wear of the insert (Fig. 21).

Regarding the performance of the cutting inserts in relation to surface defects. The A-XL cutting insert showed the best overall quality of the machined surfaces with all combinations of cutting parameters, followed by the B-XM. In contrast, the

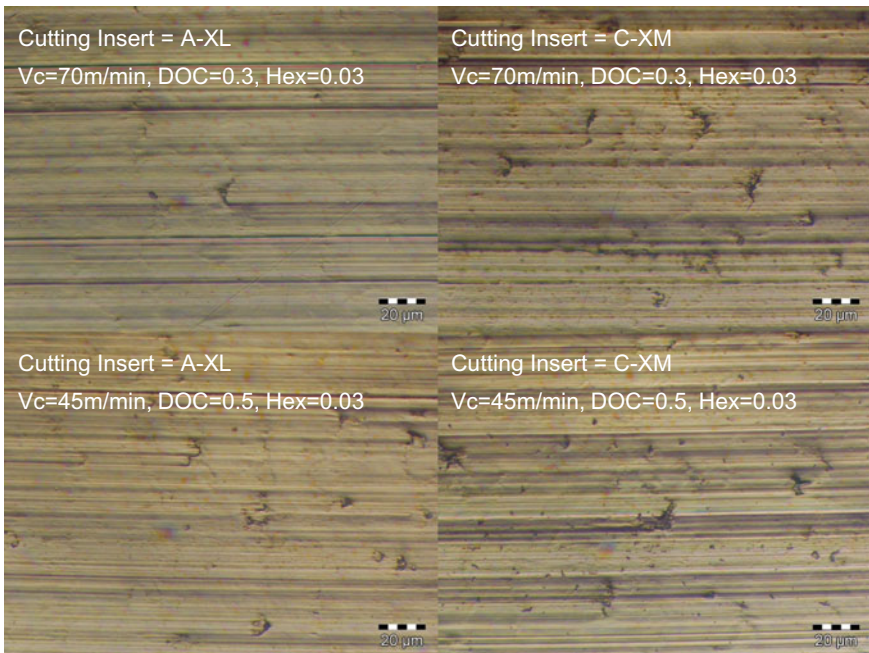


Fig. 22 Machined surface obtained with of A-XL and C-XM at different cutting parameters

surfaces that showed the greatest number of defects were those obtained with the C-XM insert. In Fig. 22 it is possible to compare the surfaces obtained with the A-XL and C-XM inserts. The performance of these inserts confirms the previous analysis of cutting forces, surfaces roughness and work-hardening tendency.

4 Conclusions

The results of milling experiments conducted on a gamma TiAl alloy for finishing cutting conditions show that for cutting forces increase of the cutting speed has a slight effect, while the depth of cut and mainly chip thickness caused a stronger impact. This trend was identified without considering the effect of cutting-edge wear.

The surface roughness R_a shows an expected dependence on cutting speed and chip thickness mainly. It was found that wear on the cutting edge improves surface roughness due to the increased contact area.

For surface hardness tendency chip thickness was revealed as the most influential parameter. An unusual trend occurred with the depth of cut. The surface work hardening tendency diminished when the depth of cut was increased from 0.3 to 0.5 mm. This improvement is probably due to the thermal softening caused by the higher DOC. Cutting speed does not cause significant differences in the explored range.

In terms of surface defects, it was not possible to obtain defect-free surfaces, but at cutting speeds of 70 m/min there is a tendency to exhibit fewer defects. This leads to the conclusion that the surface integrity can be improved by increasing cutting speed. All cutting inserts showed surfaces with higher or fewer defects according to the cutting parameters used in these trials. Consequently, a diminished surface defects would be possible. A suitable combination of cutting parameters and cutting-edge geometry must be selected for improved milling on γ -TiAl.

Summarizing, chip thickness had the greatest effect on the surface integrity variables analyzed in this research, at least in the range studied. In terms of performance, the 1010 EPL and S30T cutting inserts were the ones that provided the best surface integrity and demonstrated the potential for increased productivity.

Acknowledgements Authors acknowledge the funding of Project NORTE-01-0145-FEDER-000022—SciTech, co-financed by NORTE2020, through FEDER. Authors also acknowledge Sandvik Coromant which offered the cutting inserts.

References

1. Aspinwall, D.K., Dewes, R.C., Mantle, A.L.: The machining of γ -TiAl intermetallic alloys. *CIRP Ann. Manuf. Technol.* **54**, 99–104 (2005)
2. Beranoagirre, A., López de Lacalle, L.N.: Optimising the milling of titanium aluminide alloys. *Int. J. Mechatron. Manuf. Syst.* **3**, 425 (2010)

3. Klocke, F., Settineri, L., Lung, D., Priarone, P.C., Arft, M.: High performance cutting of gamma titanium aluminides: Influence of lubricoolant strategy on tool wear and surface integrity. *Wear* **302**, 1136–1144 (2013)
4. Priarone, P.C., Rizzuti, S., Rotella, G., Settineri, L.: Technological and environmental aspects in milling of γ -TiAl. *Adv. Mater. Res.* **223**, 340–349 (2011)
5. Mantle, A.L., Aspinwall, D.K.: Surface integrity and fatigue life of turned gamma titanium aluminide. *J. Mater. Process. Technol.* **72**, 413–420 (1997)
6. Ginting, A., Nouari, M.: Surface integrity of dry machined titanium alloys. *Int. J. Mach. Tools Manuf.* **49**, 325–332 (2009)
7. Lindemann, J., Glavatskikh, M., Leyens, C.: Surface effects on the mechanical properties of gamma titanium aluminides. *Mater. Sci. Forum* **706**, 1071–1076 (2012)
8. Beranoagire, A., López de Lacalle, L.N.N.: Grinding of gamma TiAl intermetallic alloys. In: *Procedia Engineering*, pp. 489–498 (2013)
9. Radkowski, G., Sep, J.: Surface quality of a milled gamma titanium aluminide for aeronautical applications. *Manag. Prod. Eng. Rev.* **5**, 60–65 (2014)
10. Clemens, H., Mayer, S.: Design, processing, microstructure, properties, and applications of advanced intermetallic TiAl alloys. *Adv. Eng. Mater.* **15**, 191–215 (2013)
11. Beranoagire, A., Olvera, D., López De Lacalle, L.N.: Milling of gamma titanium-aluminum alloys. *Int. J. Adv. Manuf. Technol.* **62**, 83–88 (2012)
12. Zitoune, R., Krishnaraj, V., Davim, J.P.: *Machining of Titanium Alloys and Composites for Aerospace Applications* (2013)
13. Priarone, P.C., Klocke, F., Faga, M.G., Lung, D., Settineri, L.: Tool life and surface integrity when turning titanium aluminides with PCD tools under conventional wet cutting and cryogenic cooling. *Int. J. Adv. Manuf. Technol.* **85**, 807–816 (2016)
14. Uhlmann, E., Frommeyer, G., Herter, S., Knippscheer, S., Lischka, J.M.: Studies on the conventional machining of TiAl based Alloys. In: *Ti-2003 Science and Technology 10th World Conference on Titanium*, pp. 2239–2300 (2003)
15. Aspinwall, D.K., Mantle, A.L., Chan, W.K., Hood, R., Soo, S.L.: Cutting temperatures when ball nose end milling γ -TiAl intermetallic alloys. *CIRP Ann. Manuf. Technol.* **62**, 75–78 (2013)
16. Hood, R., Aspinwall, D.K., Sage, C., Voice, W.: High speed ball nose end milling of γ -TiAl alloys. *Intermetallics* **32**, 284–291 (2013)
17. Uhlmann, E., Herter, S., Gerstenberger, R., Roeder, M.: Quasi-static chip formation of intermetallic titanium aluminides. *Prod. Eng.* **3**, 261–270 (2009)
18. Priarone, P.C., Rizzuti, S., Settineri, L., Vergnano, G.: Effects of cutting angle, edge preparation, and nano-structured coating on milling performance of a gamma titanium aluminide. *J. Mater. Process. Technol.* **212**, 2619–2628 (2012)
19. Hood, R., Aspinwall, D.K., Soo, S.L., Mantle, A.L., Novovic, D.: Workpiece surface integrity when slot milling Gamma TiAl intermetallic alloy. *CIRP Ann. Manuf. Technol.* **63**, 53–56 (2014)
20. Zhang, H., Wise, M.L.H., Aspinwall, D.K.: The machining of TiAl-based intermetallics. In: Kochhar, A.K. (ed.) *Proceedings of the Thirtieth International MATADOR Conference*, p. 739. Palgrave, London (1993)
21. Sharman, A.R.C., Aspinwall, D.K., Dewes, R.C., Bowen, P.: Workpiece surface integrity considerations when finish turning gamma titanium aluminide. *Wear* **249**, 473–481 (2001)
22. Settineri, L., Priarone, P.C., Arft, M., Lung, D., Stoyanov, T.: An evaluative approach to correlate machinability, microstructures, and material properties of gamma titanium aluminides. *CIRP Ann. Manuf. Technol.* **63**, 57–60 (2014)
23. Bentley, S.A., Mantle, A.L., Aspinwall, D.K.: Effect of machining on the fatigue strength of a gamma titanium aluminide intermetallic alloy. *Intermetallics* **7**, 967–969 (1999)
24. Mantle, A.L., Aspinwall, D.K.: Surface integrity of a high speed milled gamma titanium aluminide. *J. Mater. Process. Technol.* **118**, 143–150 (2001)
25. Novovic, D., Dewes, R.C., Aspinwall, D.K., Voice, W., Bowen, P.: The effect of machined topography and integrity on fatigue life. *Int. J. Mach. Tools Manuf.* **44**, 125–134 (2004)

26. Mathew, N.T., Vijayaraghavan, L.: Environmentally friendly drilling of intermetallic titanium aluminide at different aspect ratio. *J. Clean. Prod.* **141**, 439–452 (2017)
27. Appel, F., Paul, J.D.H., Oehring, M.: *Gamma Titanium Aluminide Alloys: Science and Technology*. Wiley-VCH Verlag GmbH & Co. KGaA, Weinheim, Germany (2011)
28. Priarone, P.C., Rizzuti, S., Rotella, G., Settineri, L.: Tool wear and surface quality in milling of a gamma-TiAl intermetallic. *Int. J. Adv. Manuf. Technol.* **61**, 25–33 (2012)
29. Vargas Pérez, R.G.: Wear mechanisms of WC inserts in face milling of gamma titanium aluminides. *Wear* **259**, 1160–1167 (2005)
30. Ge, Y.F., Fu, Y.C., Xu, J.H.: Experimental study on high speed milling of γ -TiAl alloy. *Key Eng. Mater.* **339**, 6–10 (2007)
31. Kolahdouz, S., Hadi, M., Arezoo, B., Zamani, S.: Investigation of surface integrity in high speed milling of gamma titanium aluminide under dry and minimum quantity lubricant conditions. *Procedia CIRP* **26**, 367–372 (2015)
32. Gfe Metalle und Materialien GmbH: *Advanced Materials γ -TiAl RNT650 Ingots*. 9315 (2010)
33. Weinert, K., Bergmann, S., Kempmann, C.: Machining sequence to manufacture a γ -TiAl-conrod for application in combustion engines. *Adv. Eng. Mater.* **8**, 41–47 (2006)
34. Tebaldo, V., Faga, M.G.: Influence of the heat treatment on the microstructure and machinability of titanium aluminides produced by electron beam melting. *J. Mater. Process. Technol.* **244**, 289–303 (2017)
35. Klocke, F., Lung, D., Arft, M., Priarone, P.C., Settineri, L.: On high-speed turning of a third-generation gamma titanium aluminide. *Int. J. Adv. Manuf. Technol.* **65**, 155–163 (2013)
36. Sun, S., Brandt, M., Dargusch, M.S.: Characteristics of cutting forces and chip formation in machining of titanium alloys. *Int. J. Mach. Tools Manuf.* **49**, 561–568 (2009)
37. Mantle, A.L., Aspinwall, D.K.: Cutting force evaluation when high speed end milling a gamma titanium aluminide intermetallic alloy. In: Morris, D.G., Moris, S.N., Caron, P. (eds.) *Intermetallics and Superalloys*, pp. 209–215. Wiley-VCH, Weinheim (2000)